

Removal of Fe (III) from Surface Water and Groundwater using a Cation Exchange Resin (Dowex HCR-S/S)

¹Swelam A. A., ²Y. R. Gedamy, ¹A. G. Ibrahim and ¹I. I. El-Hob

¹Department of Chemistry, Faculty of Science, Al Azhar University, Cairo, Egypt.

²Hydrogeochemistry Dept., Desert Research Center, El-Matareya, Cairo, Egypt.

Received: 27 August 2016 / Accepted: 24 Sept. 2016 / Publication date: 10 Oct. 2016

ABSTRACT

In this research, a strong cation exchange resin (Dowex HCR-S/S) with sulphonic functional groups was utilized in various conditions such as solution acidity, resin dose, contact time, initial ferric (III) concentration and temperature for iron removal from aqueous solution. The Freundlich, Langmuir, Temkin and Dubinin–Radushkevich models were applied to describe the equilibrium isotherms using nonlinear regression analysis. The results revealed that the maximum adsorption capacity (q_e) was achieved at initial iron concentration 42.75mg/l, Dowex HCR-S/S resin dosage 0.5g, after temperature 22°C. The equilibrium data fits well for the Langmuir adsorption isotherm. The Langmuir monolayer adsorption capacity of the resin was found to be 38.85mg/g. Thermodynamic parameters such as ΔG° , ΔH° and ΔS° have also been evaluated and it has been found that the sorption process was feasible, spontaneous and exothermic in nature. Activation energy (E_a) and sticking probability (S^*) of activation were also computed from linearized form of the modified Arrhenius equation. Pseudo-first-order and pseudo-second-order kinetic models were used to describe the kinetic data and the rate constants were evaluated. The result of the kinetic study shows that the adsorption of ferric (III) could be described by the pseudo-first-order equation, suggesting that the adsorption process is presumably physisorption. The adsorption process was found to be controlled by both surface and pore diffusion, with surface diffusion at the earlier stages followed by pore diffusion at the later stages. Analysis of adsorption data using a Boyd kinetic plot confirmed that external mass transfer is the rate determining step in the sorption process. So, it is concluded that Dowex HCR-S/S resin is a relatively efficient as well as the results validated the feasibility of Dowex HCR-S/S resin for highly effective removal of Fe(III) from an aqueous solution. The results obtained suggest that Dowex HCR-S/S is suitable for the remediation of Fe (III) contaminants from surface water (El Khashab canal) and groundwater (El Shorafa Village) at El Saff area, Gize, Egypt.

Key words: Removal, Fe (III), Resin, Groundwater, Surface water

Introduction

The sources of drinking water used are either surface water or groundwater sources (such as rivers, lakes, and streams). Nearly one-fifth of all water used in the world at present is obtained from groundwater (EPA, 2004).

Groundwater is considered superior in quality relative to surface water with respect to bacteriological content, turbidity, and total organic concentrations. While with respect to mineral content (hardness, iron, manganese), groundwater may be inferior and require additional treatment. Groundwater supplies are frequently pumped into the distribution system with minimal treatment (American Water Works Association, 1998). Currently, the quality of groundwater with respect to trace concentrations of organic chemicals, such as pesticides, herbicides, and solvents, is of great concern. The concentrations of these pollutants should be measured at the location of landfills, buried storage tanks, etc., for evaluation of groundwater source. Usage of ground water supplies could be optimized to provide a more reliable water source that uses the best features of both supplies (American Water Works Association, 1998).

Iron is the second most abundant metal in the earth's crust, and is mainly present in natural water in two oxidation states: Fe(II) and Fe(III). Fe(II), is essential for proper transport and storage of oxygen by means of hemoglobin and myoglobin (Safavi and Abdollahi, 1999). Iron in environmental water comes from steel tempering, coal coking and mining industries (Aksu *et al.*, 1999). Noteworthy, the water bearing formation can be consider as one of the sources for Fe(II) in the study area. Water contamination by iron

Corresponding Author: Swelam A. A., Department of Chemistry, Faculty of Science, Al Azhar University, Cairo, Egypt.
E-mail: abdelmihswelam@yahoo.com

(Fe²⁺) ions is a serious environmental problem, where iron (Fe²⁺) ions can be considered as toxic pollutants that are non-biodegradable and have environmental, public health and economic impacts.

Groundwater is the major source of domestic water for people living in rural and semi-urban areas in Egypt. Groundwater pollution by iron remains a serious issue, its presence in groundwater above a certain level makes the water unusable mainly for esthetic considerations such as discoloration, metallic taste, and odor, turbidity, staining of laundry and plumbing fixtures. Moreover, iron oxides, which are formed in reservoirs upon aerial oxidation of dissolved iron promotes growth of micro-organism in water as well as it causes: precipitation that can reduce the pipe diameter and clog valves of water distribution (Vaaramaa and Lehto, 2003). Excessive iron affects human health and causes iron toxicity because free ferrous iron react with peroxides to produce free radicals, which are highly reactive and can damage DNA, proteins, lipids, and other cellular components. Some of the problems due to iron toxicity are: anorexia, diarrhea, hypothermia, cellular death. Therefore, the World Health Organization has set a guideline value of 0.3mg/L of iron in drinking water (WHO, 1984) and many countries have adopted this value in their national drinking water quality standards including Egypt. Traditional methods used for removal of heavy metal ions from groundwater in public water supply systems in different Egyptian governorates are aeration (AL-Hobaib *et al.*, 2016) and membrane (Kumari and Tripathi, 2014), as well as oxidation with oxidizing agents such as chlorine and potassium permanganate (Armbruster *et al.*, 2015 and Huang *et al.*, 2002). Other methods available for metal ions removal from groundwater are ion-exchange (Mishra and Mahato, 2016 & Gupta and Balomajumder, 2015), adsorption on activated carbon and other adsorbents (Kohfahl *et al.*, 2016), electrocoagulation (Guzmán *et al.*, 2016) and electrosmosis techniques (Altalyan *et al.*, 2016).

The source of iron in the study area is the water bearing formation. In addition, iron can be originated from the industrial waste, where the most important pollution problem sources include the wastewater produced from the industrial complex at Helwan area in addition to the wastewater discharged into the Nile River and its canals which reached to the groundwater by seepage. On the other hand, the excessive seepage of drainage water rich in fertilizers and pesticides causes pollution for groundwater.

Noteworthy, iron concentrations more than the maximum permissible limits for drinking water (0.3mg/L) as presented by WHO, 2011, causes cooking utensils and imparts objectionable tastes and colors to foods and drinks, and their accumulation in kidney pose a serious health problem as kidney damage. So this groundwater must be treated before using for drinking and cooking.

Owing to broad applications of ferric products in many industries, ferric waste pollutes both the surface water and groundwater, and leads to a chain of environmental and health problems. In this present study, the strong cation exchange resin (Dowex HCR-S/S resin) was used as an adsorbent and it was examined for their sorption properties towards ferric (III) ions. The effect of various experimental parameters such as solution acidity, resin dose, contact time, initial ferric (III) concentration and temperature for ferric removal from aqueous solutions (single and tertiary component systems) have been investigated. Adsorption isotherms and kinetics were investigated and used to evaluate the experimental data and to elucidate the possible adsorption mechanism. The Boyd kinetic model was also tested to verify the liquid film and intra-particle diffusion mechanisms. Thermodynamic studies were also carried out to estimate the standard free energy (ΔG°), enthalpy change (ΔH°) and entropy change (ΔS°). Activation energy (E_a) and sticking probability (S^*) of activation were also computed from linearized form of the modified Arrhenius equation.

Materials and Methods

All the chemicals used were of analytical grade and used without further purification. A Dowex HCR-S/S (Na) was supplied from the Dow Chemical Company ("Dow"). The characteristics of Dowex HCR-S/S were presented in Table 1.

Adsorption study of ferric ion:

The adsorption of the ferric ion from the aqueous solution was carried out via a batch technique. At the first place, the adsorption isotherm and kinetic models, in addition to thermodynamic studies had based on studying the change of the Fe(III) solution temperatures against the operational time of initial Fe(III) concentration of 495.61mg/L ion at 22°C, 0.4g Dowex HCR-S/S resin and adsorbent/solution ratio of 10g/L were also used. For each test bottle was stirred at 150rpm with a shaking thermostat. At the completion of each time interval, the bottle was picked out from the shaker and the adsorbent was

separated from the solution by the centrifugation at 3000rpm for 5min. The solutions which contained the remains of the metal ion after the adsorption process were subjected to analysis through the AAS technique (Atomic Absorption Spectroscopy model UNICAM 929, Solar, England) to determine the adsorbed amount of the Fe(III) through the difference between its initial (C_0) and equilibrium (C_e) concentrations. The effect of the operating temperature on the efficiency of the metal ions adsorption by the Dowex HCR-S/S resin then studied in 295, 308 and 318K and, under the equilibrium time, as obtained from the prior stage. All the mentioned procedures and conditions, as described in the previous stage, had been similarly repeated in this stage of testing. Finally, the effect of the metal ion concentrations on the adsorption capability of the Dowex HCR-S/S resin was also examined. Different metal ion concentrations were applied, particularly in the range between 82.602 and 826.02mg/l. This stage was carried out at 295K while following the same experimental actions and parameters, as stated in the first stage of the adsorption investigations.

Table 1: Product Data Sheet of DOWEX™ HCR-S/S Cation Exchange Resin

Parameters		Specifications
Physical form		White to amber translucent spherical beads
Matrix		Styrene-DVB gel
Functional group		Sulfonic acid
Ionic form as shipped		Na ⁺ form
Total exchange capacity, min.	eq/L kgr/ft ³ as CaCO ₃	1.9 41.5
Bead size distribution range		
300-1,200µm, min.	%	90
< 300µm, max.	%	1
Moisture retention capacity	%	48-52
Whole uncracked beads	%	90-100
Color throw, as packaged, max.	APHA	20
Acidity range	pH	7.0-10.5
Total swelling (Ca ⁺⁺ → Na ⁺)	%	5
Particle density	g/mL	1.3
Shipping weight	g/L lbs/ft ³	800 50

The amount of the adsorbed ferric ions (q_e) in mg/g and their removal percentage of the aqueous solution were expressed according to the following equations:

$$q_e = \frac{V (C_0 - C_e)}{m} \quad (1)$$

$$\text{Adsorption (\%)} = \frac{(C_0 - C_e)}{C_0} \times 100 \quad (2)$$

Where C_0 and C_e are the initial concentration and the concentration at equilibrium of Fe(III) in mg/L, respectively, m is the mass of the adsorbent and V is the volume of the solution.

Effect of initial iron concentration:

Concentration dependency study was carried out at different initial iron concentrations vary from 42.75 mg/l to 538.65mg/l at 298K and 0.4g in 50ml solution, and the results are shown in Fig.1. From the obtained results, it is observed that the adsorption capacity (q_e) increases with increase of the initial iron concentration and the maximum adsorption capacity (q_e) was achieved at higher concentration (538.65 mg/l) and remains constant. This may be explicable as follows: the adsorbent sites eventually become saturated with adsorbed cations and then further addition of sorptive ions would not be expected to increase the amount adsorbed significantly (Liu and Gao, 2015).

Effect of adsorbent dosage:

The adsorption capacity and removal rate of Fe(III) as a function of resin dosage are presented in Fig. 2. The obtained results showed that, the larger dosage of a resin would increase the removal process of

ferric ion from aqueous solution, and the maximum removal rate was determined to be 99.93% for 0.5g Dowex HCR-S/S resin per 50ml ferric solution. This could be explained by the fact that the higher the dose of adsorbent in the solution, the more active sites for Fe(III). Whereas the number of available adsorption sites increases by an increase in adsorbent dose and these leads to increase in removal efficiency (Ho *et al.*, 1995). It is evident from the figure that the adsorption capacity (q_e) increases with increase in adsorbent dose up to a particular region and then reaches an equilibrium level (no significance change) at higher doses. This may be due to the overlapping of active sites at higher dosage. So, this trend could be due to the formation of adsorbent aggregates at higher adsorbent concentrations, which in turn could reduce the effective surface area available for the adsorption (Soumya *et al.*, 2015). So, 0.5g was considered as an optimum dose and was used for further study.

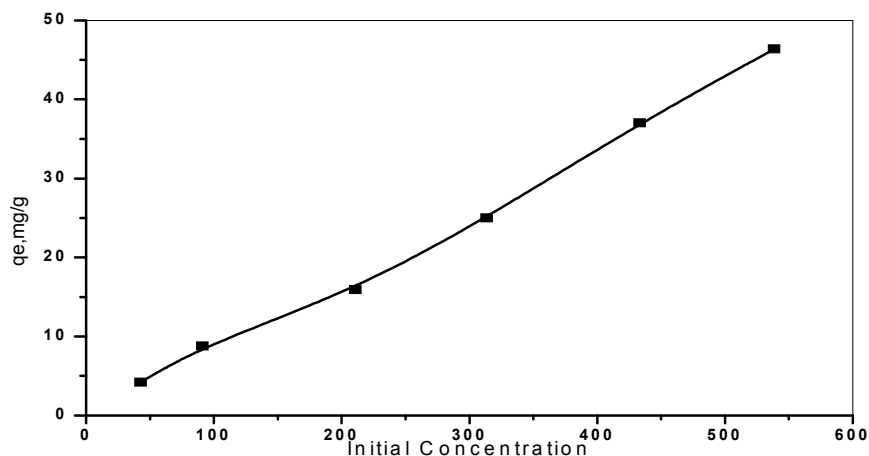


Fig. 1: Effect of different initial ferric concentrations on the maximum uptake

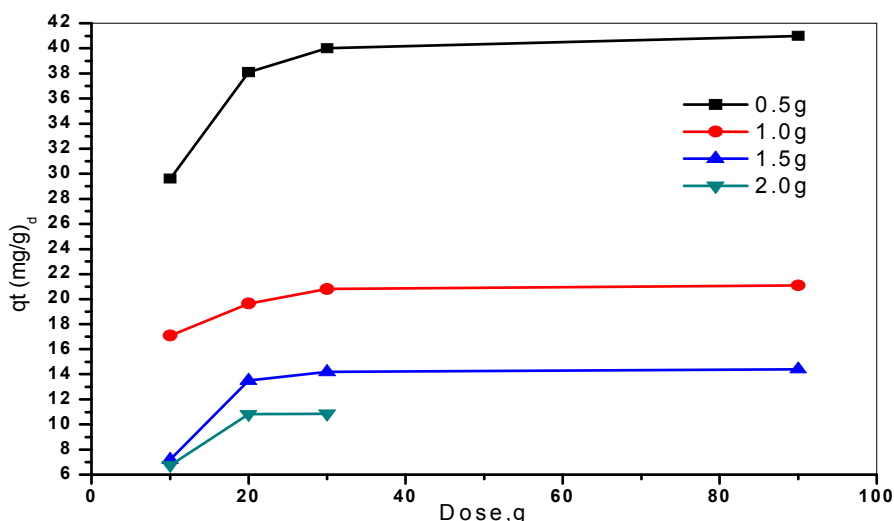


Fig. 2: Effect of the resin dosage on the ferric uptake

Effect of contact time:

Kinetics experiments were carried out to determine the effect of contact time on adsorption procedure. The effect of contacting time on the uptake of Fe(III) by resin was carried out by placing 0.5g of dry resin in a flask containing 50ml of Fe(III) solution at an initial concentration of 410.4mg/l and without change in the pH value (pure aqueous solution). The contents of the flask were placed on a shaker

at 150rpm and at temperature 22 ± 1 °C. One milliliter of the solution was taken at different time intervals and used to determine the residual concentration of Fe(III).

As is shown in Fig. 3, the adsorption was faster during the first 20min, the efficiency of the resin toward the ferric ion was 35.3mg/g (86.01%), while after that the extent of adsorption slowly approached equilibrium for the metal ions. After 30min, apparent equilibrium was achieved 38.7mg/g (94.29%). No further adsorption occurred even after 2h of contact time, which indicated that the adsorption of metal cation on the surface of the resin could be taken in a single step with no complexity (Tiwari *et al.*, 2007). The following experimental contact time was designed to be 2h to make sure the establishment of equilibrium. In the first 20min, the rate of adsorption was apparently fast, which can be explained that the available adsorption sites were sufficient compared with the density with the bare surface of the adsorbent in the beginning. As the process goes on, the adsorption sites became saturated gradually. The uptake rate was controlled by the rate at which the adsorbate transported from the exterior to the interior sites of the adsorbent particles, so the adsorption became much slower (Yu *et al.*, 2001) and (Shi *et al.*, 2009).

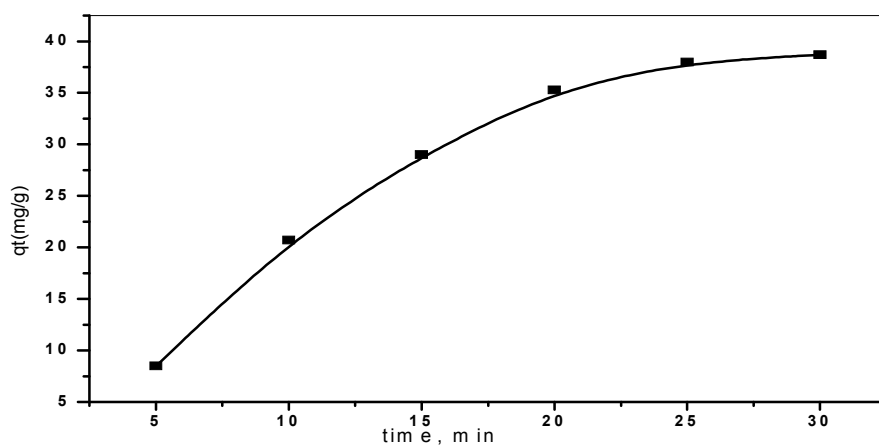


Fig. 3: Effect of contact time on the uptake of Fe (III) at 410.4 mg/l and 22°C

Effect of solution acidity:

The uptake of Fe(III) by the Dowex HCR-S/S resin was studied at different solution acidity values (0.001, 0.002, 0.004, 0.006, 0.008, 0.01, 0.05, 0.1 and 0.5M HCl). The solution acidity was studied using hydrochloric acid solutions. 0.5g of investigating resin was placed in a series of flasks. To each flask 50mL of Fe(III) solution (410.4 mg/g) was added. The contents of each flask were shaken for 180min on a shaker at 150rpm and at temperature 22 ± 1 °C at the desired solution acidity. The resin was separated from the solution by filtration. Then the residual concentration of Fe(III) was estimated as above.

The uptake capacity of Fe(III) was gradually decreased with increase the solution acidity. In such acidic medium the uptake may be explained to proceed through repulsion forces between the aqua-iron complex with high positive charge $(\text{Fe}(\text{H}_2\text{O})_4(\text{OH})_2\text{Fe}(\text{H}_2\text{O})_4)^{+4}$ and the resin active sites $(-\text{SO}_3\text{H})$ (Pramauroa *et al.*, 1992). It is noteworthy to refer that; the above positively charged (+4) aqua complex of iron compete the positive charges of sulphonic groups in acid medium. This type of competition increases at higher concentration of H^+ (higher solution acidity values) giving a lower uptake value (Fig. 4). On the other hand, the uptake capacity of Fe(III) was gradually increased with decrease the solution acidity. In lower acidic medium, the negative charges of hydroxyl groups were increase, leads to a higher ferric uptake. This may be explained to proceed through a decrease in the repulsion forces between the aqua-iron complex with high positive charge and the resin active sites $(-\text{SO}_3\text{H})$ (Pramauroa *et al.*, 1992). It is noteworthy to refer that, the above positively charged (+4) aqua complex of iron less competes and overcome the protonation of the sulphonic groups (Namdeo and Bajpai 2008). This type of competition decreases at lower concentration of H^+ (lower solution acidity) giving a higher uptake value (Fig. 4).

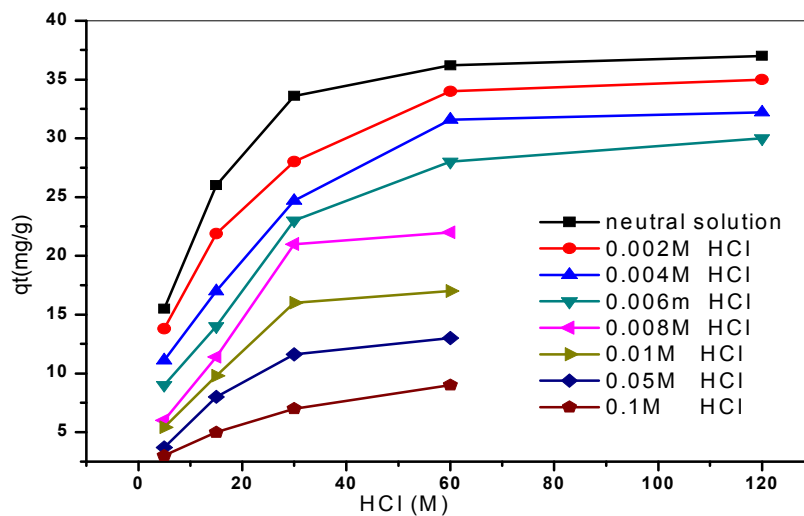


Fig. 4: Hydrochloric acid effects on the ferric uptake at 430.35 mg/l and 22°C

The distribution ratio (K_d):

Distribution ratio K_d for ferric ions was determined by the batch method at different temperature systems. The distribution ratio, K_d (L/mg), is defined as the ratio of metal ion concentration on the resin to that in the aqueous solution (Equation 3) and can be used as a valuable tool to study Fe(III) mobility.

$$K_d = q_e/C_e \tag{3}$$

Various portions of (400mg each) the resin were taken in Erlenmeyer flasks and mixed with 50ml of different metal ion solutions in the aqueous medium and subsequently shaken for 24h in temperatures controlled shaker at 295, 308 and 318K to attain the equilibrium.

Fig. 5 shows that the distribution ratio (K_d) values increase with the increase in temperatures of ferric solutions. High values of the distribution ratio at 318K (Asif and Shaheen, 2013), indicate that the metal has been retained by the solid phase through sorption reactions, while lower values of K_d at 295K, indicate that a large fraction of the metal remains in solution. The rapid metal sorption has significant practical importance, as this will facilitate with the small amount of resin to ensure efficiency and economy.

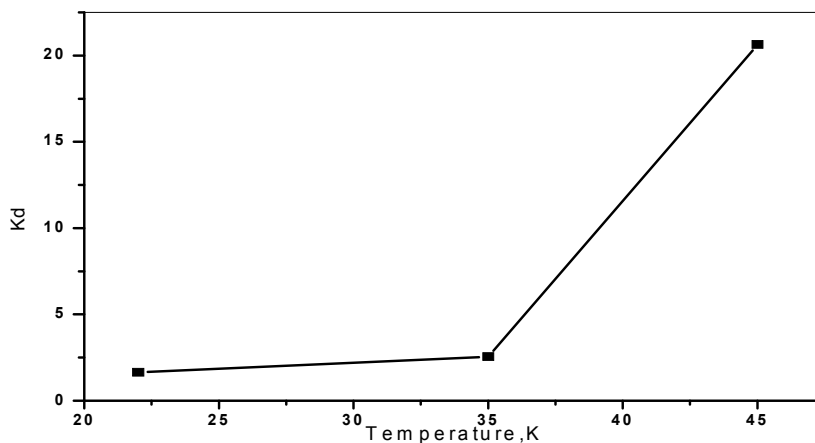


Fig. 5: Distribution coefficients of ferric at different temperatures

Adsorption isotherms:

Isotherms provide fundamental physiochemical data to evaluate the sorption capacity. In the present study, four isotherms were employed to analyze the experimental results at different temperatures 298, 308 and 318K. The collected data during this stage were then fitted to the Freundlich (Freundlich, 1918 and Zhu *et al.*, 2015), Langmuir (Langmuir, 1918 and Barnabas *et al.*, 2016), Temkin (Temkin and Pyzhev, 1940 & Zhou *et al.*, 2016) and D-R (Dubinin and Radushkevich, 1947 & Fan *et al.*, 2016) formulas (Equations 5 and 6) in order to determine the adsorption nature and the isothermal parameters, the applied equations were in the linear form.

Freundlich isotherm model:

The Freundlich model is used to describe the sorption characteristics of heterogeneous surfaces, taking into account the interactions between the adsorbed molecules. The used equation is the following empirical equation;

$$q_e = K_f C_e^{1/n} \quad (4)$$

Where K_f (mg/g) is the Freundlich isotherm constant indicating adsorption capacity and n is the adsorption intensity while $1/n$ is a function of the strength of the adsorption, C_e is the equilibrium concentration of adsorbate (mg/L) and q_e is the amount of adsorbate per adsorbent at equilibrium (mg/g). The logarithmic form of Freundlich is defined as:

$$\ln q_e = \ln K_f + 1/n \ln C_e \quad (5)$$

From the plot of $\ln q_e$ versus $\ln C_e$, (Fig. 6) K_f and n were calculated and explored in Table 2. The n value gives an indication of the favorability of the adsorption process. A value of $n < 1$ indicates a favorable adsorption, while $n > 1$ indicates a cooperative adsorption. In this study the value of n is 53.53 (as shown in Table 2) indicating an unfavorable adsorption process of Fe(III) on the resin.

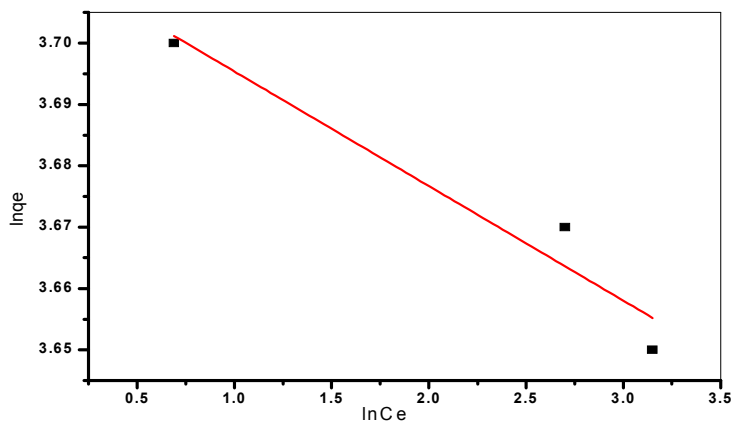


Fig. 6: The Freundlich plot of ferric adsorption

Langmuir isotherm model:

Langmuir model introduces a concept of forming a single (monolayer) surface phase on energetically homogeneous surfaces of the adsorbent. The linear Langmuir equation is given by the following equation;

$$\frac{C_e}{q_e} = \frac{1}{k_L q_m} + \frac{C_e}{q_m} \quad (6)$$

Where k_L is Langmuir equilibrium constant (L/mg) related to the affinity of adsorption sites, and q_m (mg/g) is the maximum theoretical monolayer adsorption capacity, C_e is the equilibrium concentration

(mg/L) of Fe(III) in solution and q_e is the amount of ferric ions adsorbed (mg/g) at equilibrium. (Fig. 7) depicts the plot of C_e/q_e versus C_e . The R^2 value of 0.99988 certifies that the data fitted the Langmuir Isotherm model. The values of Langmuir constants q_m (38.85) and k_L (6.55) were computed from the slope and intercept of the plot (as shown in Table 2). The maximum adsorption capacity q_m was agreed well with the experimental value (q_{exp} , 38.7). This other support on the fitting the adsorption process with the Langmuir model.

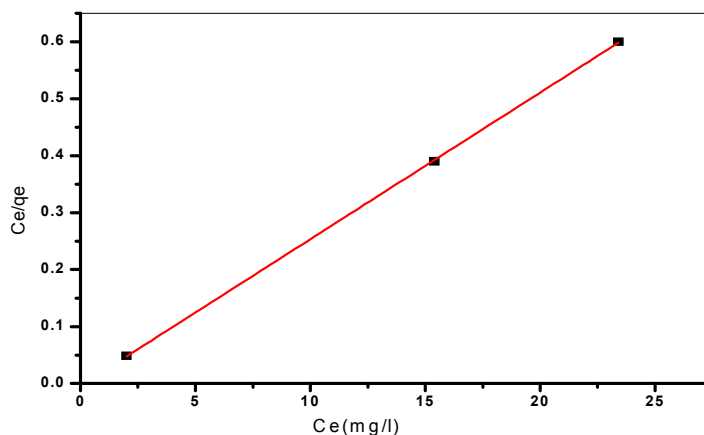


Fig. 7: The Langmuir plot of ferric adsorption

The characteristic parameter of the Langmuir isotherm is illustrated in terms of dimensionless equilibrium parameter R_L , also known as separation factor, defined by this equation;

$$R_L = \frac{1}{1 + k_L C_0}$$

Where, C_0 is the initial solute concentration. The value R_L gives an indication of the type of the isotherm and the nature of the adsorption process. It indicates whether the adsorption nature is either unfavorable ($R_L > 1$), linear ($R_L = 1$), favorable ($0 < R_L < 1$) or irreversible ($R_L = 0$). The R_L value of 0.000372, indicate the favorable nature of the adsorption.

Table 2: Adsorption isotherm parameters for ferric in aqueous media.

Freundlich			Langmuir			
n	$K_F(\text{mol}^{1-n}\text{L}^n/\text{g})$	R^2	$Q_{\max}(\text{mg}/\text{g})$	$K_L \text{ L}/\text{mg}$	R_L	R^2
53.53	41.02	0.89066	38.85	6.55	0.000372	0.99988
Temkin			D-R			
$A_T(\text{L}/\text{min})$	$B_T(\text{J}/\text{mol})$	R^2	$B(\text{mol}^2/\text{kJ}^2)$	X_m g/g	$E(\text{kJ}/\text{mol})$	R^2
2.76×10^{-19}	0.982	0.9608	3.55375	38.83	0.3751	0.70061

The Temkin model:

The Temkin model takes into account the adsorbent–adsorbate interactions and assumes a linear decrease in the energy of adsorption with surface coverage. The Temkin isotherm model is expressed by:

$$q_e = B_T \ln A_T + B_T \ln C_e \quad (7)$$

Where $B_T = RT/b$, R is the universal gas constant (8.314 J/mol/K), T is the absolute temperature (degrees in Kelvin) and A_T is the equilibrium binding constant and B_T is corresponding to the heat of sorption. The isotherm constants were determined (A_T is 2.755×10^{-19} , B_T is 0.9817). The linear plot for The Temkin adsorption isotherm (Fig. 8) fits quite well with an R^2 of 0.9608 as shown in Table 2.

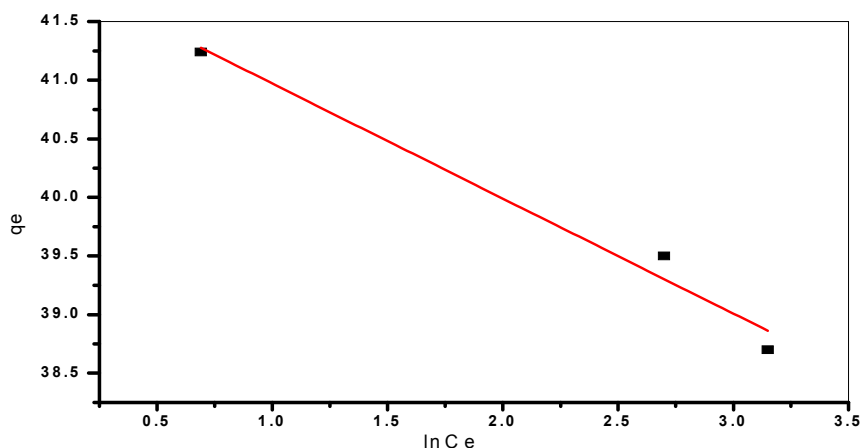


Fig. 8: The Temkin plot of ferric adsorption

Dubinin–Radushkevich (D–R) isotherm:

Dubinin–Radushkevich isotherm assumes a fixed volume or ‘sorption space’ close to the sorbent surface and determines the heterogeneity of sorption energies within the sorption space and is applied in the linearized form of the equation as;

$$\ln q_e = \ln X_m - \beta \epsilon^2 \tag{8}$$

Where q_e is in mg/g (described earlier), X_m represents the maximum sorption capacity of sorbent (mg/g) and β ($\text{kJ}^2 \text{mol}^{-2}$) is a constant with dimensions of energy. The Polanyi sorption potential ϵ , which is the amount of energy required to pull a sorbed molecule from its sorption site to infinity may be evaluated by using relationship.

$$\epsilon = RT \ln \left(1 + \frac{1}{C_e} \right) \tag{9}$$

Where, R is a gas constant in $\text{J mol}^{-1} \text{K}^{-1}$, ‘ T ’ is the temperature in Kelvin, C_e (mg/l) is as mentioned earlier. In the plot of $\ln q_e$ versus ϵ^2 yield coefficient of determinations (Fig. 9) and the result of X_m (38.83) computed from the slope and intercept of respective plots are documented in Table 2. R^2 values (0.70061) showed that the D–R model poor fit to the experimental data of iron adsorption. The mean free energy of sorption (E) can be defined as the free energy change when one mole of ion is transferred from infinity in solution to the sorbent (Senthil Kumar *et al.*, 2011). It can be calculated using the relationship

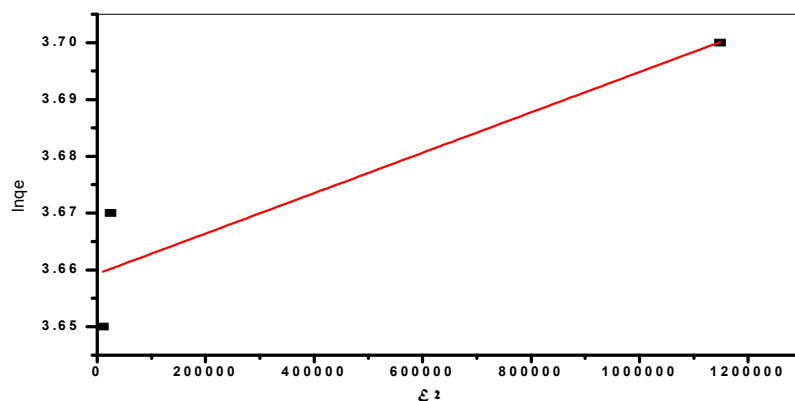


Fig. 9: The D-R plot of ferric adsorption

$$E = 1/\sqrt{2B} \tag{10}$$

The E value in our studies shows a high value (0.375 kJ mol⁻¹), indicating the physical nature of the ferric adsorption processes onto the resin.

Adsorption kinetics:

The adsorption kinetics is useful to foretell the rate of adsorption and provide valuable data for understanding the mechanism of the sorption. Here, two kinetic models of Fe(III) adsorption were evaluated by applying: the pseudo-first order (Lagergren, 1898 and Ding *et al.*,2016) and the pseudo-second order (Ho *et al.*,1995 and Lin *et al.*, 2016). The pseudo-first-order model was applied to depict the adsorption of liquid/solid system based on solid capacity.

Equation for Lagergren's pseudo-first order kinetics is presented in the following form:

$$\ln(q_e - q_t) = \ln q_e - k_1 t \tag{11}$$

Where q_t and q_e stand for the amounts of Fe(III) (mg/g) adsorbed at a time t and at equilibrium, respectively, while k_1 stands for the first order rate constant (min⁻¹). The values of k_1 and $q_{e, cal}$, calculated from the plots of $\ln(q_e - q_t)$ versus t (Fig.10).

Comparing the experimental equilibrium adsorption value (Table 3), $q_{e, exp}$ (38.7) with calculated values of $q_{e, cal}$, (102.514), it is clear that there is no agreement between the values. On the other hand, the obtained correlation coefficient (R^2) for the first model show good linearity (0.93639), thereby indicating the adsorption process follow the Lagergren's pseudo-first model which implies the physical nature of this process at 295K.

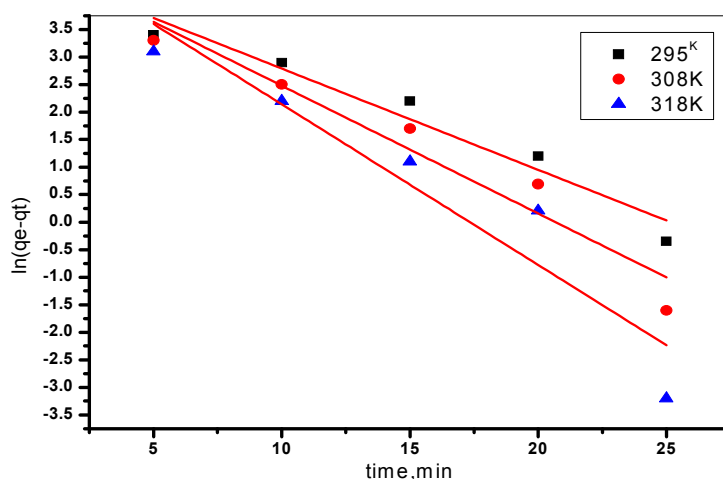


Fig. 10: The pseudo-first-order plot of ferric adsorption

The following adsorption kinetic rate equation is used to express the pseudo-second-order kinetic model.

$$dq_t/dt = k_2(q_2 - q_t)^2 \tag{12}$$

Where k_2 denotes the rate constant of the pseudo-second-order adsorption (g/mg min), while q_e and q_t are the respective adsorbed amount (capacity) of Fe(III) at equilibrium and at time t .

The linear form of the pseudo-second order can be expressed as follow:

$$t/q_t = (1/k_2 q_2^2) + (1/q_2)t \tag{16}$$

A plot of t/q_t against t provided the k_2 values (Fig. 11) as listed in (Table 3).

The values of the correlation coefficient, R^2 (0.43791) at 298K, indicate that the adsorption process was deviated from the pseudo-second-order kinetic model, and the Fe(III) ions were adsorbed on the resin via physical interaction.

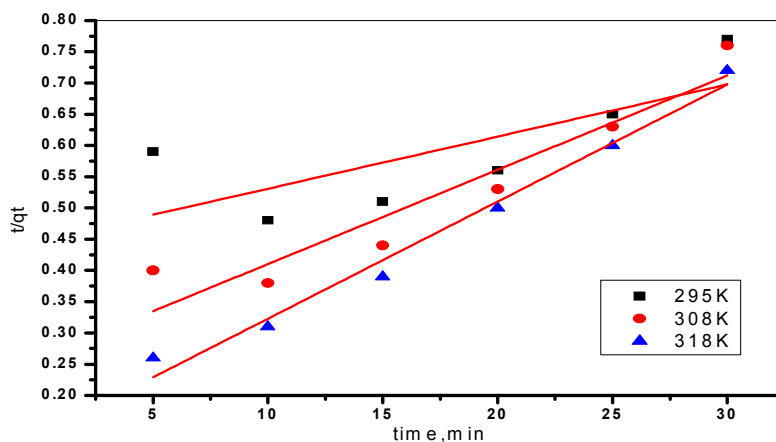


Fig. 11: The Pseudo-second-order plot of ferric adsorption at different temperature

Table 3: Kinetic parameters for ferric ion in aqueous media.

Temp. (K)	Pseudo first-order model			Pseudo second-order model		
	q_e 1 cal mg/g	K_1 min ⁻¹	R^2	q_e 2 cal mg/g	K_2 (g/mgmin)	R^2
295 K	102.52	0.184	0.93639	119.9	15.55×10^{-5}	0.43791
308 K	121.63	0.2322	0.91644	66.27	8.78×10^{-4}	0.88006
318 K	157.43	0.2918	0.86837	53.36	25.95×10^{-4}	0.98045
Temp. (K)	Intra-particle diffusion model			Film diffusion		
	$K_{id} t$ (mg/g)(min) ^{0.5}	C (mg/g)	R^2	D_i (cm ² /s)	R^2	
295 K	5.18435	5.06299	0.6515	9.44×10^{-3}		0.89011
308 K	4.38847	11.7238	0.5482	11.27×10^{-3}		0.94654
318 K	3.45506	19.6428	0.4915	12.68×10^{-3}		0.84730

Adsorption mechanism:

It is most important to predict the rate-limiting step in an adsorption process to understand the adsorption mechanism associated with the phenomena. For a solid-liquid sorption process, the solute transfer is usually characterized by either external mass transfer (boundary layer diffusion) or intra-particle diffusion or both. The following three steps can describe the adsorption dynamics (Özacar and Sengil, 2005; Seliem *et al.*, 2016 and Acharya *et al.*, 2009).

- 1- The movement of adsorbate molecules from the bulk solution to the external surface of the adsorbent (film diffusion).
- 2- Adsorbate molecules move to the interior part of the adsorbent particles (particle diffusion).
- 3- Sorption of the solute on the interior surface of the pores and capillary spaces of adsorbent (sorption).

The intra-particle diffusion model:

This model is normally used for a deeper understanding of the adsorption mechanism. A plot of q_t versus $t^{0.5}$ should be a straight line when the adsorption process is controlled by the intra-particle diffusion where the adsorbate ions diffuse in the intra-particle pore of the adsorbent. However, more than one step could govern the process if the data exhibit multi-linear plots. The intra-particle diffusion co-efficient, k_{id} , can be determined by fitting the experimental data in the intra-particle diffusion model (Weber *et al.*, 1963) expressed as follow:

$$q_t = k_{id}t^{1/2} + C \tag{17}$$

Where k_{id} is the intra-particle diffusion rate constant (mg/g min^{1/2}), C is the intercept (mg/g). Our experimental data revealed that the plot of q_t versus $t^{1/2}$ is multi-linear (Fig.12), indicating that three steps are involved in the process (adsorption) and intra-particle diffusion is not the only rate-limiting step. The intra-particle diffusion constant values are 9.62502 (k_{id}), 10.4847 (C) and 0.94293 (R^2) at 298K as shown in Table 3. However, it was observed that, there are three linear portions that explain the adsorption stages; these are the external mass transfer at initial period, intra-particle diffusion of Fe(III) on the resin, and adsorption on the interior sites.

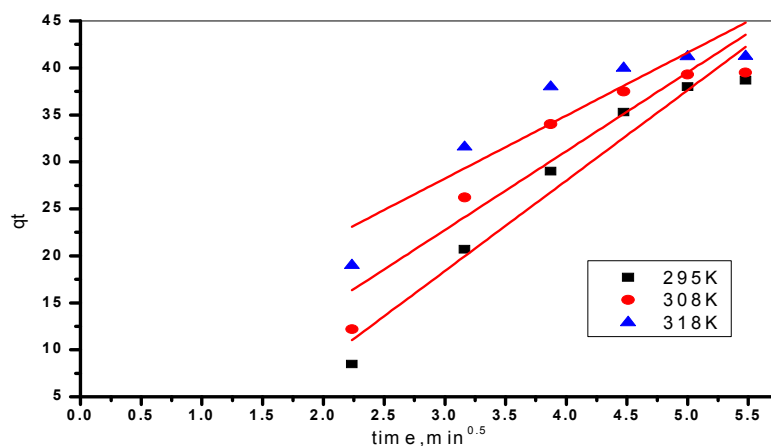


Fig. 12: The Intra-particle diffusion plot of ferric adsorption

Boyd kinetic model:

The third step in the adsorption dynamics of Fe(III) ion is assumed to be very rapid and it can be considered negligible. For design purposes, it is required to distinguish between film diffusion and particle diffusion of adsorbate molecules. In order to identify the slowest step in the adsorption process, Boyd kinetic equation (Boyd *et al.*, 1947) was applied, which is expressed as follow;

$$F = 1 - \frac{6}{\pi^2} \exp(-Bt) \tag{18}$$

and

$$F = \frac{q_t}{q_e}$$

Where q_e is the amount of Fe(III) adsorbed at equilibrium (mg/g) and q_t represents the amount of ferric adsorbed at any time t , F represents the fraction of ferric (III) adsorbed at any time t , and Bt is a mathematical function of F (Reichenberg, 1953).

The plot of Bt against time t can be employed to test the linearity of the experimental values. If the plots are linear and pass through the origin, then the slowest step in the adsorption process is the internal diffusion. It was observed that the plots are linear (Fig.13), but do not pass through the origin, suggesting that the adsorption process is controlled by film diffusion. The calculated B values were used to calculate the effective diffusion coefficient, D_i (m²/s) using the following relationship:

$$B = \frac{\pi^2 D_i}{r^2} \tag{19}$$

Where D_i is the effective diffusion coefficient of Fe(III) in the Dowex HCR-S/S resin surface and r is the radius of the resin particles. The D_i values were found to be 9.44×10^{-3} , 11.27×10^{-3} and 12.92×10^{-3} at different temperatures 298, 308 and 318K, respectively (as shown in Table 3). A Boyd kinetic plot confirms that the external mass transfer was the slowest step involved in the adsorption process (Boyd *et al.*, 1947).

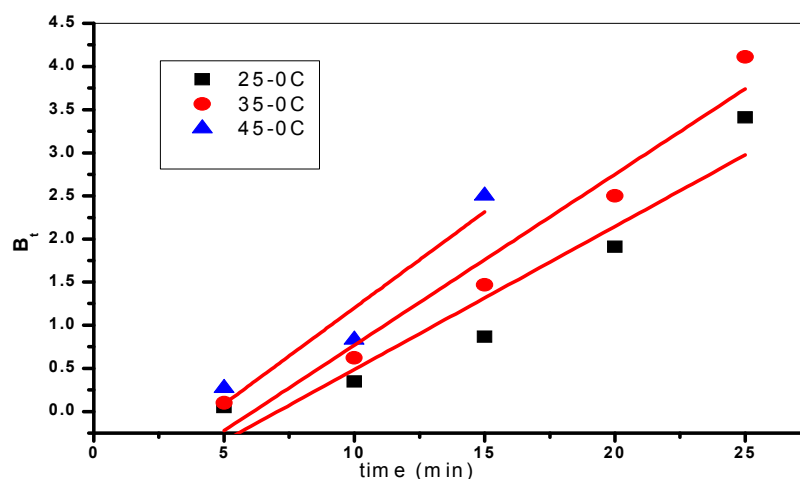


Fig. 13: Boyd plot for Fe (III) adsorption at 0.5g/50ml, 410.4 mg/l and at different temperatures

Effect of temperature and evaluation of thermodynamic parameters:

Effect of temperature on the Fe(III) removal was studied in the range of 22 to 45°C while keeping all other parameters constant. The results summarized in (Fig.14), indicate that the adsorption rate increases with an increase in temperature, and indicate that the process is apparently endothermic and governed by chemical forces. This may also be the result of the decreased desorption process of an increase in thermal energy of the adsorbate.

On the other hand, enhancement of the adsorption capacity of the resin at higher temperatures may be attributed to the activation of the adsorbing surface and increase in the mobility of metal ions. Also, this fact demonstrated an endothermic sorption process.

The removal percentage of Fe(III) onto the adsorbent (Fig.14) was increased with increase of temperatures ranged from 94.29% to 97.46% by the Dowex HCR-S/S resin, with increase in temperature from 295 to 318 K. This may be due to the formation of new active sites in the adsorbents to increase in temperature, activation of the adsorbing surface and increase in the mobility of metal ions.

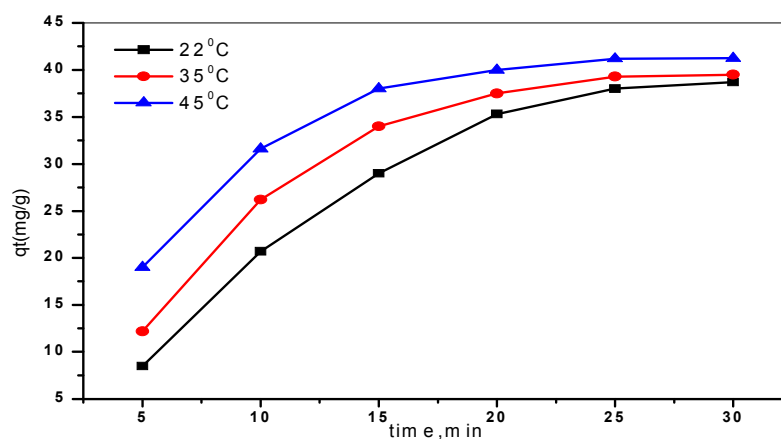


Fig. 14: The temperature effects on the uptake of ferric ions

The thermodynamic parameters ΔG° (standard free energy), ΔH° (enthalpy change) and ΔS° (entropy change) were calculated to determine the nature of the adsorption. The experimental data obtained at different temperatures were used to calculate the thermodynamic parameters by a plot of $\ln K_d$ versus $1/T$ (Fig. 15), by using the linear Van't Hoff equation.

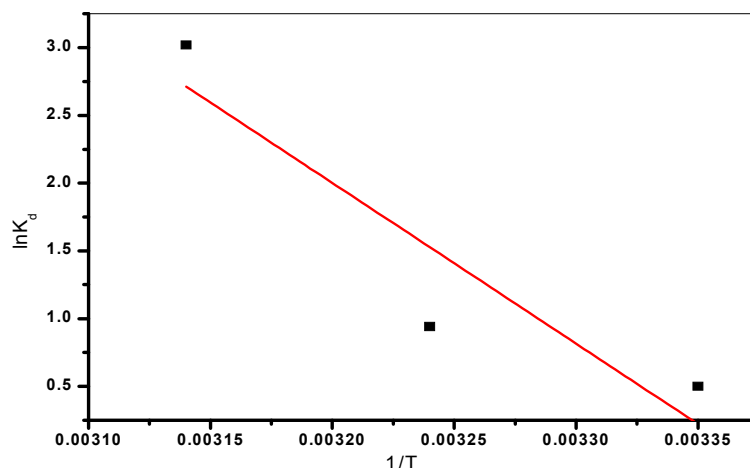


Fig. 15: The Van't Hoff plot of ferric adsorption

$$\ln K_d = \frac{\Delta S}{R} - \frac{\Delta H}{RT} \quad (20)$$

$$\Delta G = \Delta H - T\Delta S \quad (21)$$

Where R is the gas constant of 8.314 J/mol K, T is the absolute temperature in K. and $K_d = q_e/C_e$ (L/mg) is the standard thermodynamic equilibrium constant.

The increase of negative values of ΔG° value with increasing temperature indicates that adsorption of the ion on the adsorbent becomes favorable at a higher temperature (Table 4). The positive standard enthalpy change ΔH° of 98.66 kJ/mol suggests that the adsorption of Fe(III) on the resin is an endothermic process. The positive standard entropy change of 332.35 J/mol K encourages the adsorption process. The increase in randomness at the solid-solution interface during the fixation of Fe(III) on the active motifs of the resin is a consequence of loss of water molecules from the hydration shells of Fe(III).

Table 4: Thermodynamic parameters for ferric in aqueous media.

T(K)	ΔG° kJ/mol	ΔS° J/mol K	ΔH° kJ/mol	S*	E _a kJ/mol
295	-197.70	332.35	98.662	1.04.X10 ⁻¹⁸	96.167
308	-201.03				
318	-204.35				

In order to further support the assertion that the adsorption is the predominant mechanism, the values of the activation energy (E_a) and sticking probability (S^*) were estimated from the experimental data. They were calculated using a modified Arrhenius type equation related to surface coverage (Singh and Das, 2013) as expressed in the following equations (22 and 23);

$$\theta = 1 - \frac{C_e}{C_0} \quad (22)$$

$$S^* = (1 - \theta) \exp\left(-\frac{E_a}{RT}\right) \quad (23)$$

The sticking probability, S^* , is a function of the adsorbate/adsorbent system under consideration and is dependent on the temperature of the system. The parameter S^* indicates the measure of the potential of an adsorbate to remain on the adsorbent indefinitely. It can be expressed as in Table (4). The effect of temperature on the sticking probability was evaluated throughout the temperature range from 298 to 318 K by calculating the surface coverage at the various temperatures. Table (4) also indicated that the values of

$S^* \leq 1$ (1.04×10^{-18}) for the Dowex HCR-S/S resin, hence the sticking probability of the Fe(III) ion onto the adsorbent systems is very high.

Adsorption activation energy:

The magnitude of E_a gives an indication of the type of the adsorption process, physical or chemical. The physisorption process is readily reversible, equilibrium is attained rapidly and thus the energy requirements are small, ranging between 5 and 40 kJ/mol. The chemisorption mechanism is specific and involves stronger forces, and thus requires large activation energy ranging from 40 to 800 kJ/mol (Anirudhan and Radhakrishnan, 2008 & Chakraborty *et al.*, 2011). The high activation energy E_a of 96.167 kJ/mol, as calculated from the slope (Fig.16), reflects the chemical nature of the adsorption process.

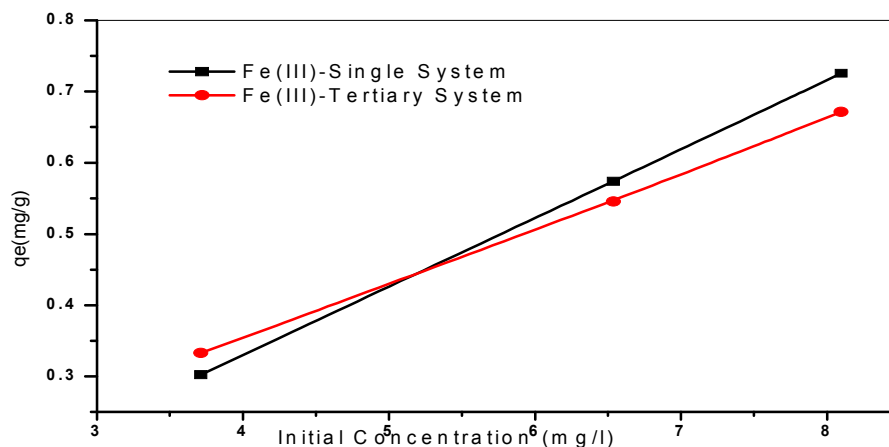


Fig. 16: The Arrhenius plot of ferric adsorption

Competitive adsorption study:

In nature, numerous heavy metal ions are often mixed together to form multi-component systems (Lee *et al.*, 2015). There is a need to investigate the simultaneous removal of many co-existing heavy metal ions. Competitive adsorption of Fe(III), Cu(II) and Zn(II) by the Dowex HCR-S/S resin in synthetic single and tertiary systems is shown in Fig.17.

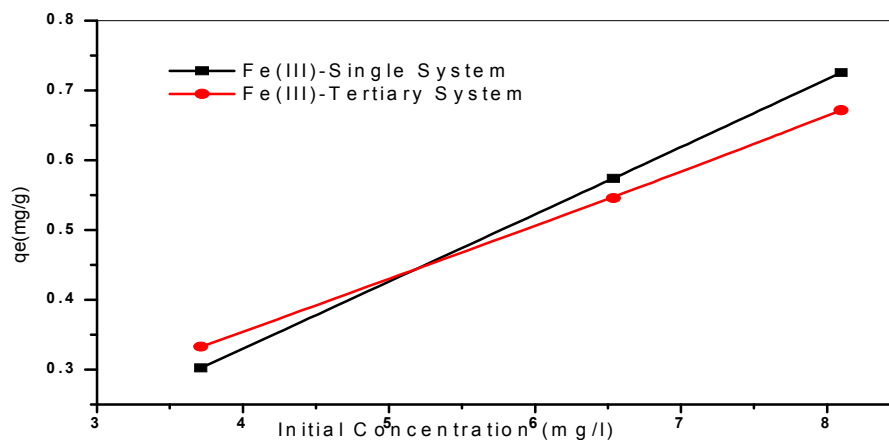


Fig. 17: Effects of different concentrations of Fe(III) in single and tertiary systems on ferric uptake

All metal ion removal performance of 0.5g the Dowex HCR-S/S cation exchange resin was evaluated as a function of 50ml of the initial ferric ion concentrations from 3.712 to 8.097ppm in neutral aqueous solutions. The Fe(III) ion was analyzed by flame atomic absorption spectrometry as above. In this study, the adsorption time was fixed at 120min because the adsorption of Fe(III) ion onto the Dowex HCR-S/S resin sufficiently reached an equilibrium state based on the contact time dependency test. As illustrated in Fig.17, the Fe(III) adsorption capacity depended on the initial metal ion concentration. Notably, when the initial metal ion concentration ranged from 3.712 to 8.097ppm, the adsorption capacity of the Fe(III) ion shows significantly increased with the increase of the initial Fe(III) ion concentrations but the removal percentage showed decreases in the system. In the range of tested concentrations, the Fe(III) ion could bind to the abundant adsorption sites on the surface of the Dowex HCR-S/S resin, leading to the distinctively increased adsorptivity of the resin.

Multi component adsorption studies are important to assess the degree of interference posed by common metal ions present in wastewaters or natural water (groundwater). The sorption dynamics of the mixture was probed using q_e'/q_e ratios, where the prime denotes the presence of other metal ions. In general, three possible types of behavior are exhibited in multicomponent adsorbates–adsorbents (Mahamadi and Nharingo, 2010). $q_e'/q_e > 1$, synergism (the effect of the mixture is greater than that of the individual adsorbates in the mixture); $q_e'/q_e < 1$, antagonism (the effect of the mixture is less than that of each of the individual adsorbates in the mixture) and $q_e'/q_e = 1$, non-interaction (the mixture has no effect on the adsorption of each of the adsorbates in the mixture).

The tri-metal sorption of Fe(III), Cu(II) and Zn(II) ions in aqueous systems by Dowex HCR-S/S resin was investigated to establish the effect of the presence of three metal ions on the sorption of each one of them in different concentrations.

The q_e'/q_e ratios for the sorption of one metal Fe(III) at different concentrations namely, 3.712, 6.537 and 8.097ppm in the presence of other metals Cu(II) at different concentrations namely, 3.648, 6.592 and 9.331ppm as well as Zn(II) at different concentrations namely, 1.68, 4.871 and 5.353ppm are shown in Fig.7. The ratios of Ferric ion at different concentrations were all < 1 , indicating that the adsorption of the metal was depressed by the presence of other metal ions in the tertiary solutions; hence the effect of the mixtures seemed to be antagonistic. The q_e'/q_e ratios for the sorption of Fe(III) ion in the presence of Cu(II) and Zn(II) ions were 0.4751, 0.6821 and 0.7996 at the three concentrations, respectively. These values indicate that there was a significant difference in the magnitude of suppression of Ferric ion uptake in the presence of both copper and zinc ions. Thus, these results show that in all cases, there was an inhibitory effect of one metal on binding of the other metal. Interestingly, the overall adsorption capacities of the Dowex HCR-S/S resin for Fe (III) ion in the tertiary system at the different concentrations were 0.3326, 0.5457 and 0.6717 mg/g, respectively, and were lower than the adsorption capacities of Fe (III) (0.3021, 0.5737 and 0.7275 mg/g, respectively), in the single component systems. For that reason, the adsorption sites of Fe(III) ion may partially be overlapped with those of Cu(II) and Zn(II) ions in tertiary system. Overall, the sorption order in the tertiary system was found to be $Cu > Fe > Zn$.

Field study:

The suitability of Dowex HCR-S/S resin was tested with a field samples taken in the study area. About 0.5 g of adsorbent was added to 50 ml of water sample and the contents were shaken with constant time 60 min at room temperature (25^o). As shown in Table 5, the results indicated that the removal percentage reached about 84.1 to 91.77% for surface water and groundwater, respectively, which reveal that Dowex HCR-S/S resin can be effectively employed for removing the Fe (III) ion from surface water and groundwater.

Table 5: Field trial results of Dowex HCR-S/S resin on surface water and groundwater samples in the study area

Sample Name	Iron concentration before treatment	Iron concentration after treatment	Removal percentage (%)
Surface water			
El Khashab canal	38.93 ppm	6.188 ppm	84.1
Groundwater			
El Shorafa Village	4.7 ppm	0.387 ppm	91.77

Conclusion:

The present study showed that the Dowex HCR-S/S resin as a strong cation exchange resin can be used as an adsorbent for the removal of ferric (III) from aqueous solutions whether; it was single or tertiary systems. The removal of Fe(III) ions from aqueous solutions strongly depends on the solution pH, resin dose, contact time, initial ferric(III) ion concentration and temperature. It was observed that the adsorption was concentration dependent and the maximum adsorption of 98.24% occurred for an initial ferric (III) ion concentration of 42.75 mg/l. With increase in the resin dose increase in ferric (III) adsorption was found to increase owing to a corresponding increase in the number of active sites. The adsorption was rapid and equilibrium was achieved within 25 min. The percentage removal of ferric (III) ions increased with increase in temperature. The data obtained from the thermodynamic study at different temperatures were used to calculate the thermodynamic quantities such as ΔG° , ΔH° and ΔS° of adsorption. The results indicated that ferric (III) adsorption onto Dowex HCR-S/S resin was found to be spontaneous and exothermic. The equilibrium data have been analyzed using Langmuir, Freundlich, Temkin and Dubinin–Radushkevich adsorption isotherms. The characteristic parameters for each isotherm and related correlation coefficients were determined. The Langmuir adsorption isotherm was demonstrated to provide the best correlation for the adsorption of ferric (III) onto the resin. The maximum monolayer adsorption capacity of the Dowex HCR-S/S resin was found to be 38.85mg of ferric (III)/0.5g of the resin. The adsorption kinetics of ferric (III) onto the Dowex HCR-S/S resin was studied by using pseudo-first-order and pseudo-second-order equations. The kinetic results showed that ferric (III) – Dowex HCR-S/S resin system cannot be described by the pseudo-second-order equation. Since the correlation coefficients obtained for this equation was lower than those of pseudo-first-order equation, and calculated q_e values were found to deviate considerably from the experimental values. The pseudo-first-order equation provided the best correlation of the experimental data. The external mass transfer controlled the ferric (III) removal at earlier stages and intra-particle diffusion at later stages of adsorption. A Boyd kinetic plot confirms that the external mass transfer was the slowest step involved in the adsorption process. Based on the results obtained from these studies, it can be concluded that since the Dowex HCR-S/S resin is an easily, available, low-cost adsorbent and has a considerable high adsorption capacity, it may be treated as an alternative adsorbent for treatment of wastewater containing ferric (III) ions. The results obtained suggest that Dowex HCR-S/S is suitable for the remediation of Fe (III) contaminants from surface water (El Khashab canal) and groundwater (El Shorafa Village) at El Saff area, Gize, Egypt.

References

- Acharya, J., J.N. Sahu, C.R. Mohanty and B.C. Meikap, 2009. *Chem. Eng. J.*, 149: 249-262.
- Aksu, Z., A. Calik, A.Y. Dursun and Z. Demircan, 1999. *Process Biochem.*, 34: 483-491.
- AL-Hobaib, A.S., K.M. AL-Sheetan and L. El Mi, 2016. *Materials Science in Semiconductor Processing*, 42(1): 107-110.
- Altalyan, H.N., B. Jones, J. Bradd, L.D. Nghiem and Yasir M. Alyazichi, 2016. *J. Water Process Eng.*, 9: 9-21.
- American Water Works Association, 1998. *Water Quality and Treatment*, fourth Edition.
- Anirudhan, T.S. and P.G. Radhakrishnan. *J. Chem*, 2008. *Thermodynamics*, 40: 702-709.
- Armbruster, D., O. Happel, M. Scheurer, K. Harms and T.C. Schmidt, 2015. *Heinz-Jürgen Brauch; Water Res.*, 79: 104-118.
- Asif, A.K. and S. Shaheen, 2013. *Solid State Sci.*, 16: 158.
- Barnabas, M.J., S. Parambadath, A. Mathew, S. Park, A. Vinu and Chang-Sik Ha, 2016. *J. Solid State Chemistry*, 233: 133-142.
- Boyd, E.G., A.W. Adamson and L.S. Myers, 1947. *J. Am. Chem. Soc.*, 69: 2836-2848.
- Chakraborty, S., S. Chowdhury and P.D. Saha, 2011. *Carbohydrate Polym.*, 86: 1533-1541.
- Ding, Z., X. Hub, Y. Wand, S. Wang and B. Gao, 2016. *J. Industr. Eng. Chem.*, 33: 239-245.
- Dubinin, M.M. and L.V. Radushkevich, 1947. *Chem. Zentr*, 1: 875-889.
- EPA's, *Watershed Information Network*, 2004: 354-367.
- Fan, H., W. Sun, B. Jiang, Q. Wang, Da-Wu Li, C. Huang, K. Wang, Z. Zhang and W. Li' *Chem*, 2016. *Engin. J.* 286: 128-138.
- Freundlich, H.J. *Am.*, 1918. *Chem. Soc.*, 40: 1361-1403.
- Gupta, A. and C. Balomajumder, 2015. *Groundwater for Sustainable Development*, 1: 12-22.

- Guzmán, A., J.L. Nava and O. Coreño, 2016. *Israel Rodríguez, Silvia Gutiérrez; Chemosphere*, 144: 2113-2120.
- Ho, Y.S., D.A. John Wase and C.F. Forster, 1995. *Water Res.*, 29: 1327-1332.
- Huang, K., G.E. Hoag, P. Chheda, B.A. Woody and G.M. Dobbs, 2002. *Advances in Environ. Res.*, 7: 217-229.
- Kumari, M. and B.D. Tripathi, 2014. *Ecological Engineering*, 62: 48-53.
- Kohfahl, C., D.S. Navarro, J.A. Mendoza, I. Vadillo and E. Giménez- Forcada, 2016. *Science of The Total Environ.*, 544: 874-882.
- Lagergren S. Handlingar, 1898. 24(4): 1-39.
- Langmuir, I.J., 1918. *Am. Chem. Soc.*, 40: 1361-403.
- Lee, C., J. Jeon, M. Hwang, K. Ahn, C. Park, 2015. Jae-Woo Choi and Sang-Hyup Lee. *Chemosphere*, 130: 59-65.
- Lin, K.A., Y. Liu and S. Chen, 2016. *J. Colloid and Interf. Sci.*, 461: 79-87.
- Liu, Q. and Y. Gao, 2015. *LWT - Food Science and Technology*, 63: 1245-1253.
- Mahamadi, C. and T. Nharingo, 2010. *Bioresour. Technol.*, 101: 859-864.
- Mishra, T. and D.K. Mahato, 2016. *J. Environ. Chem. Eng.*, 4: 1224-1230.
- Namdeo, M. and S.K. Bajpai, 2008. *Colloid Surf. A*, 320: 161-168.
- Özacar, M. and I.A. Sengil., 2005. *Process Biochem.*, 40: 565-572.
- Pramauroa, E., B. Alessandra, E. Barnib, G. Viscardib and W.L. Hinzec, 1992. *Colloid Surf.*, 63: 291-300.
- Reichenberg, D.J., 1953. *Am. Chem. Soc.*, 75: 589-597.
- Safavi, A. and H. Abdollahi, 1999. *Microchem. J.*, 63: 211-217.
- Senthil Kumar, P., S. Ramalingam, S. Dinesh Kirupha, A. Murugesan, T. Vidhyadevi and S. Sivanesan, 2011. *Chem. Eng. J.* 167(15): 122-131.
- Shi, T., S. Jia, Y. Chen, Y. Wen, C. Du, H. Guo and Z. Wang. *J. Hazard*, 2009. *Mater.*, 169: 838-846.
- Seliem, M.K., S. Komarneni and R. Mostafa Abu Khadra, 2016. *Microporous and Mesoporous Mater.*, 224: 51-57.
- Singh, B. and S.K. Das, 2013. *Colloids and Surf. B: Biointer.*, 107: 97-106.
- Soumya, G.N., M. Manickavasagam, P. Santhanam, S. Dinesh Kumar and P. Prabhavathi, 2015. *African Journal of Biotechnology*, 14(16): 1393-1400.
- Temkin, I.M. and V. Pyzhev, 1940. *Acta Physiochem. SSR*, 12: 217-222.
- Tiwari, D., H.U. Kim and S.M. Lee, 2007. *Sep. Purif. Technol.*, 57: 11-16.
- Vaaramaa, K. and J. Lehto, 2003. *Desalination*, 155: 157-170.
- Weber, W.J., J.C. Morris and J. Sanit, 1963. *Eng. Div. Am. Soc. Civ. Eng.*, 89: 31-60.
- WHO, 1984. *Guidelines for Drinking Water Quality, Recommendations*, vol. 1, World Health Organization, Geneva, Switzerland, p: 79.
- WHO, 2011. *Guidelines for Drinking-water Quality. Recommendations*. 4thed. Geneva, World Health Organization.
- Yu, B., Y. Zhang, A. Shukla, S.S. Shukla and K.L. Dorris, 2001. *J. Hazard. Mater.*, 84: 83-94.
- Zhou, G., J. Luo, C. Liu, L. Chu, J. Ma, Y. Tang, Z. Zeng and S. Luo, 2016. *Water Research*, 89: 151-160.
- Zhu, Y., N. Gao, Q. Wang and X. Wei, 2015. *Colloids and Surf. A: Physicochem. Eng. Aspects*, 468: 114-121.